4-Dimensional geoelectrical monitoring of slopes that affect transport infrastructure

Jessica HOLMES[1], Jonathan CHAMBERS[2], Paul WILKINSON[2], Philip MELDRUM[2], Jimmy BOYD[2], Mihai CIMPOIASU[2], Paul WILLIAMSON[2], David HUNTLEY[3], Sebastian UHLEMANN[4], Shane DONOHUE[5]

[1]Newcastle University, Newcastle upon Tyne, United Kingdom
[2]British Geological Survey, Nottingham, United Kingdom
[3]Geological Survey of Canada, Vancouver, Canada
[4]Lawrence Berkeley National Laboratory, US
[5]University College Dublin, Dublin, Republic of Ireland
Corresponding author: Jessica Holmes (jessica.holmes@newcastle.ac.uk)

Abstract

Slope instability on transport networks globally is a growing issue, particularly in light of environmental change, and it presents social, economic, and environmental challenges. Consequently, there is an increasing need for improved management and monitoring on the transport network to maintain serviceability. Timelapse geoelectrical imaging is a novel method for monitoring transport infrastructure assets, offering an alternative to traditional time- and cost-intensive methods. Here, we present results from the Proactive Infrastructure Monitoring and Evaluation (PRIME) System, developed by the British Geological Survey. PRIME allows for remote near-real time monitoring of subsurface moisture conditions using an electrical resistivity tomography (ERT) instrument with telemetric control and data retrieval to reduce the need for repeat field visits. This is beneficial as it enables daily delivery of information on critical sites located in very remote locations and the therefore reduces the risk of exposure of rail personnel at site for more traditional on-site walk over inspections. 4-D ERT monitoring results are presented for two field sites: (1) Old Dalby, a railway embankment in Leicestershire, UK, for which vegetation type and distribution significantly influences near surface resistivity and moisture dynamics; (2) the Ripley landslide, a natural slope in British Columbia, Canada, where freeze-thaw cycles dominate the seasonal changes in resistivity. Following the application of petrophysical relationships developed in the laboratory to the ERT models, the models are interpreted in the context of moisture content and soil suction changes in time and space – two factors that are important for slope stability. Complex, seasonally variable hydrogeological pathways are revealed at both study sites, highlighting the utility of near surface geophysics for monitoring critical earthworks assets and natural slopes affecting infrastructure in two different environments.

Keywords: Slope Stability, Electrical Resistivity Tomography, Petrophysical relationships

1. Introduction

There is increasing demand on the transport network globally due to economic development, and population growth, and as slope failure is also increasing in response to environmental change, there is growing interest from stakeholders in monitoring slopes on the transport network (Mattsson and Jenelius, 2015). Traditionally, slopes on the transport network are monitored using visual surveys and discrete-point geotechnical investigations, which often fail to capture the complexity of heterogeneous slopes, many of which were constructed rapidly during the industrial revolution. A shift toward novel technologies for monitoring slopes is recommended by a recent report on earthworks management (Mair et al., 2021). Near-surface geophysics provides one such opportunity for slope monitoring, allowing data acquisition from a large volume of the subsurface, relatively quickly and inexpensively compared with traditional monitoring techniques.

Electrical Resistivity Tomography (ERT) is used increasingly for monitoring unstable slopes (Chambers et al., 2014; Perrone et al., 2014; Gunn et al., 2015; Holmes et al., 2020; Holmes et al., 2022). Electrical resistivity is sensitive to changes in moisture content, changing conductivity of the pore fluid (Waxman and Smits, 1968), and temperature (Hayley et al., 2007), so it can be used to monitor changes in these parameters through time and space. Given that moisture content is also a key control on slope stability, ERT is a useful tool in slope stability assessment (Uhlemann et al., 2017). Related to moisture content, soil suction is also a key control on slope stability, affecting shear strength and effective stress (Fredlund et al., 1978). As such, ERT has the potential to estimate soil suction indirectly (Holmes et al., 2022).

Here, laboratory-derived petrophysical relationships that relate resistivity to moisture content directly are presented. They are applied to ERT models to provide insight into changes in moisture content through time. Results are presented from two sites; one a natural landslide in British Columbia, Canada, where freeze-thaw cycles dictate changes in resistivity, and one a railway cutting in the United Kingdom that demonstrates the importance of vegetation for controlling moisture dynamics.

2. Methodology

2.1 ERT Monitoring and data processing

A 4-D ERT monitoring system, PRIME (Proactive Infrastructure Monitoring and Evaluation) (Holmes et al., 2020), was installed on the Ripley Landslide, British Columbia, Canada, and the Old Dalby railway cutting, Leicestershire, United Kingdom. PRIME consists of sensor (electrode) arrays connected to the system, which takes electrical resistivity measurements at set time intervals and sends the data to a remote server via an internet connection, allowing sites to be monitored continually through time to develop 4-D ERT datasets. To ensure accurate models of the subsurface were produced from the ERT data, data points with high contact resistances were removed, and measurements with reciprocal errors >5% were removed (Tso et al., 2017). Data were processed in a 3-D inversion using Res3DInv (Loke, 2017). Table 1 describes the set-up of the PRIME system and the data processing used for each site.

PRIME Details	Ripley Landslide	Old Dalby Railway cutting
Data acquisition	2 years	2 years
Electrode arrays	2; one 90 m with 45 electrodes, one 54 m with 27 electrodes	5; two 90 m with 91 electrodes, three 20 m with 19 electrodes
Electrode spacing	2 m	1 m
Electrode type	Buried rod	Buried rod
Array type	Dipole-dipole	Dipole-dipole
Inversion program	Res3DInv	Res3DInv
Inversion constraints	L1 norm spatial smoothness constraint; L2 norm temporal smoothness constraint	L2 norm spatial smoothness constraint; L1 norm temporal smoothness constraint

Table 1: PRIME ERT details for each field site.

2.2 Developing Petrophysical Relationships

Direct relationships between soil moisture, soil suction, and electrical resistivity for each lithological unit at the field sites (Figure 1) were developed in the laboratory, using a modified HYPROP2 (METER Group) (Holmes et al., 2022), as shown in Figure 2. No relationship was developed for Unit 8 of the Ripley Landslide as the material was too coarse to enable a cohesive sample to be obtained. A sample was cut using an electrically non-conductive polyether ether ketone (PEEK) container (250 cm^3) (undisturbed samples for the Ripley Landslide, and reconstituted samples for Old Dalby owing to site inaccessibility). Four equally spaced electrodes (1 cm in length) were inserted into the sample and connected to a ES-2 sensor (METER Group), which was modified to allow conductivity measurements to be taken in a different geometric set-up than its original design. Samples were saturated and moisture content, suction, and electrical conductivity were measured simultaneously as the samples dried through a complete drying cycle.

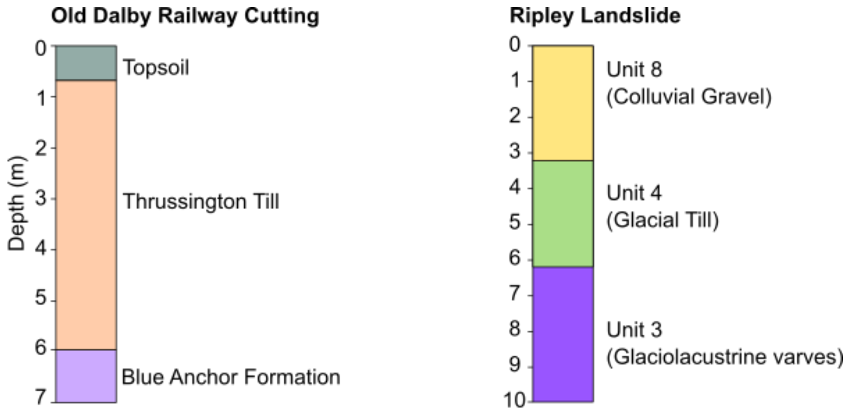

Figure 1: Sediment logs from the location of the PRIME monitoring at the Ripley Landslide and the Old Dalby Railway Cutting.

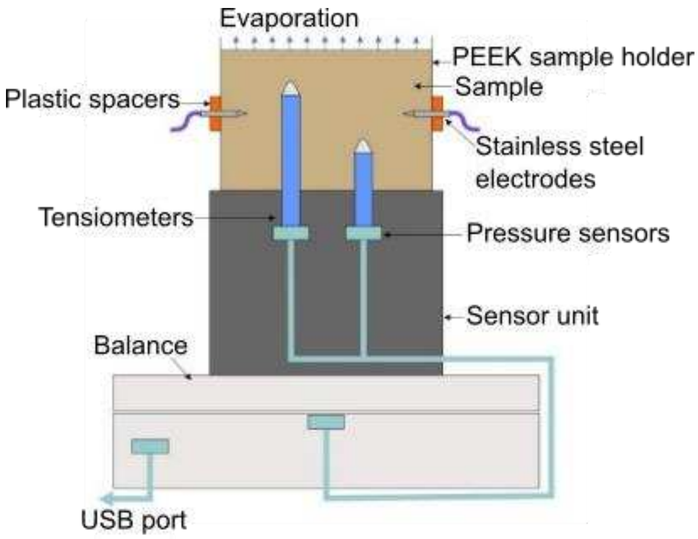

Figure 2: Modified HYPROP 2 set-up. (After Holmes et al., 2022).

A modified Waxman-Smits model was fitted to the resistivity and moisture content data measured in the laboratory, as in Uhlemann et al. (2017):

$$\rho(GMC) = F\left(\frac{(1-\varphi)D_g GMC}{\varphi D_w}\right)^{-n}\left(\sigma_w + B_{ws}\left[\frac{(1-\varphi)D_g C}{100\varphi}\right]\left[\frac{\varphi D_w}{(1-\varphi)D_g GMC}\right]\right)^{-1} \quad [1]$$

Where, *F* is a formation factor, φ is porosity, *Dg* is grain density (g cm-3), D_w is water density (g cm^{-3}), *n* is a saturation exponent, σ_w is the pore water conductivity (S m-1), and *C* is cation exchange capacity (meq/100 g). The average cation mobility, B_{ws} (S cm^3 m^{-1} meq^{-1}), was estimated from the empirical fit given by Waxman and Smits (1968). Each parameter was measured in the laboratory, with the exception of *F* and *n*, which were fitted and B_{ws}, which was estimated (Waxman and Smits, 1968):

$$(B_{ws} = 4.6(1 - 0.06\, Exp\left[-\frac{\sigma_w}{1.3}\right]). \quad [2]$$

Waxman-Smits models were fitted to the data from each lithological unit tested in the laboratory to convert electrical resistivity to gravimetric moisture content. The resulting models were used for the calibration of the ERT models generated from data from the PRIME systems. The parameters used in this calculation for each lithological unit are shown in Table 2.

Waxman-Smits Model		F (-)	n (-)	Φ (-)	D_g (g/cm^3)	D_w (g/cm^3)	σ_w (S/m)	B_{ws} (S cm^3 m^{-1} meq^{-1})	C (meq /100 g)
Ripley Landslide	Unit 3 High GMC	35.576	3.481	0.37	2.53	1	0.033	1.91	17.4
	Unit 3 Low GMC	25.364	2.272	0.37					
	Unit 4 High GMC	22.224	2.333	0.48	2.53	1	0.0528	1.95	17
	Unit 3 Low GMC	19.600	3.256	0.35					
Old Dalby Railway Cutting	Thrussington Till	7.992	2.244	0.35	2.65	1	0.031	1.91	10.8
	Blue Anchor	5.565	2.709	0.49	2.72	1	0.249	2.32	21.9

Table 2: Parameters used in the fitting of Waxman-Smits models to the laboratory data (Holmes et al., 2022; Holmes et al., in review).

3. Results and Discussion

3.1 Ripley Landslide – Freeze-thaw behaviour

ERT models were calibrated using the petrophysical relationships presented in Eq 1, using parameters from Table 2, with a different relationship applied to each lithological unit (Figure 1). GMC was isolated on the calibrated PRIME model for the head scarp zone of the Ripley Landslide and the non-head scarp zone and the average GMC of the cells in each zone was calculated. GMC through time is shown in Figure 3, alongside weather conditions.

Most of the changes in GMC occurred in the head scarp zone, with relatively little change in the rest of the slope. GMC increased in the head scarp zone following the onset of the snowmelt period each year as air temperature rose above 0 °C in the spring (March–April), and in response to positive effective rainfall. Following propagation of the wetting front down the slip face of the Ripley Landslide, GMC remained elevated compared with that of the slide mass. Increased GMC is likely to cause a reduction in matric suction and normal effective stress, increasing the likelihood of failure. Additionally, the magnitude of change in GMC in the head scarp zone was greater than in the non-head scarp zone (GMC values ranged from 0.35 to 0.49 g/g and 0.1 to 0.16 g/g respectively). This cyclic wetting and drying can result in shrink-swell behaviour and therefore further increasing susceptibility to failure due to a decrease in shear strength.

Additionally, due to the shrink-swell and freeze-thaw movement that occurs in the head scarp zone, tension cracks are prevalent in this area. This resulted in a quicker response in this zone to rainfall events, as the tension cracks provide a preferential pathway for moisture movement. There was little response to changes in effective rainfall in the subsurface outside of the head scarp zone. This is because changes in electrical resistivity in the very near surface occurred predominantly in Unit 8 (Figure 1), for which no GMC data is available. Therefore, changes in GMC presented here are seasonal, and the effects of individual rainfall events are not observed, except for in the head scarp zone.

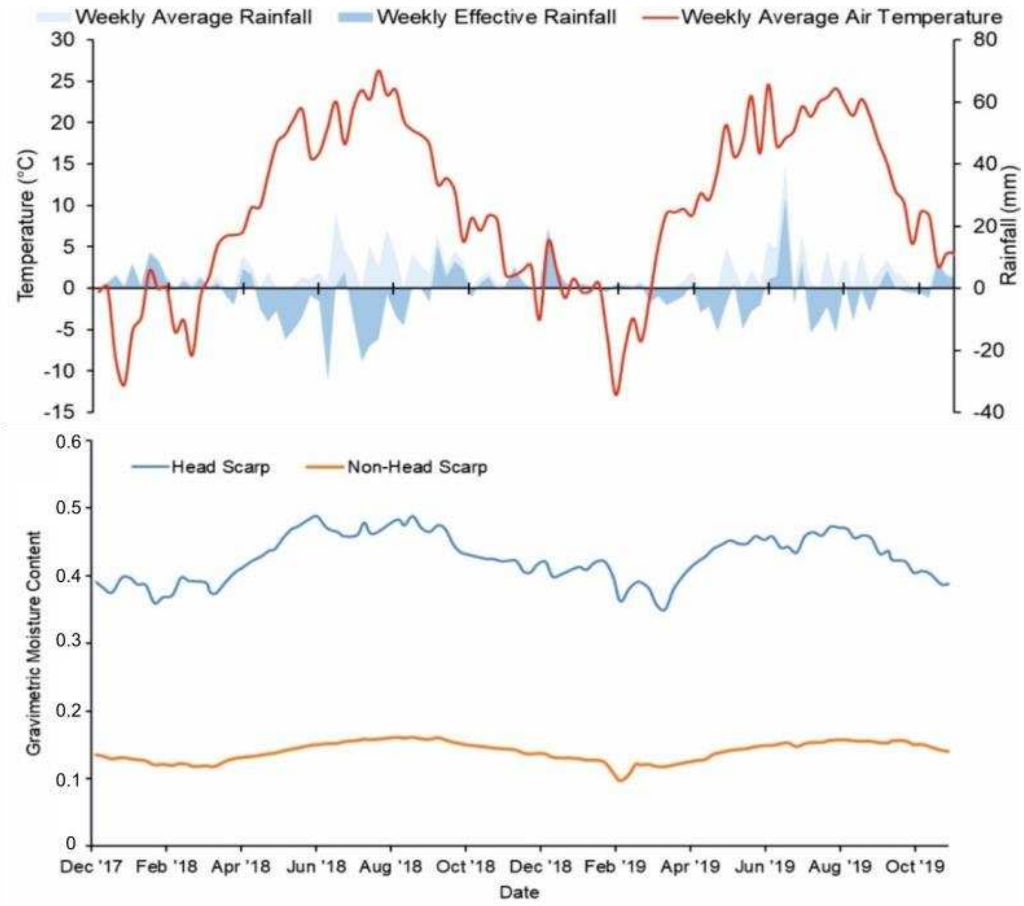

Figure 3: Average gravimetric moisture content through time for head scarp and non-head scarp regions of the upper 5 m of the PRIME monitored areas of the landslide based on laboratory calibrations of ERT model, shown with weather data including air temperature, rainfall, and effective rainfall. (After Holmes et al., 2022).

3.2 Old Dalby Railway Cutting – Vegetation

ERT models of the Old Dalby railway cutting were calibrated using the petrophysical relationships presented in Eq 1, using parameters from Table 2, with a different relationship applied to each lithological unit (Figure 1). Discrete volumes within the ERT models were identified from which the average GMC of the model cells in grassed areas of the slope and wooded areas of the slope respectively were identified. Figure 4 shows the average GMC of each of these regions over the monitoring period, along with weather data and volumetric moisture content (VMC) data from sensors installed on the slope.

Seasonal changes in GMC were observed in the wooded areas, with lower GMC in summer, when temperatures were higher, and higher GMC in winter when higher intensity and longer duration rainfall events are common. However, these seasonal changes were not observed in the grassed regions of the slope, where GMC remained elevated above that of the wooded regions all year round. This indicates that the presence of vegetation exacerbates the subsurface response to seasonal changes in weather conditions. The role of vegetation in controlling spatial distributions of soil moisture is greater during the summer due to increased plant activity during this time due to increased air temperature and longer daylight hours. In winter, plant activity (evapotranspiration) is reduced, which explains the reduction in the difference in GMC spatially between wooded and grassed areas during this time.

Therefore, vegetation type is an important consideration for transport infrastructure asset stability. In wooded areas, the GMC ranged between 0.095 and 0.130 g/g, whereas for grass, the range was much narrower, ranging between 0.124 and 0.138 g/g. While the presence of roots can increase slope stability due to increased cohesion, repeated wetting and drying cycles can exacerbate shrink-swell behaviour, and a reduction in shear strength (Khan et al., 2019). Indeed, near to the Old Dalby PRIME installation, surface signs of slope instability are observed in the wooded zone, with tension cracks appearing. This highlights the need to consider vegetation in the assessment of slope stability on the transport network. Due to the shrink-swell behaviour associated with trees and the high levels of soil moisture associated with grasses, a combination of vegetation types is suggested.

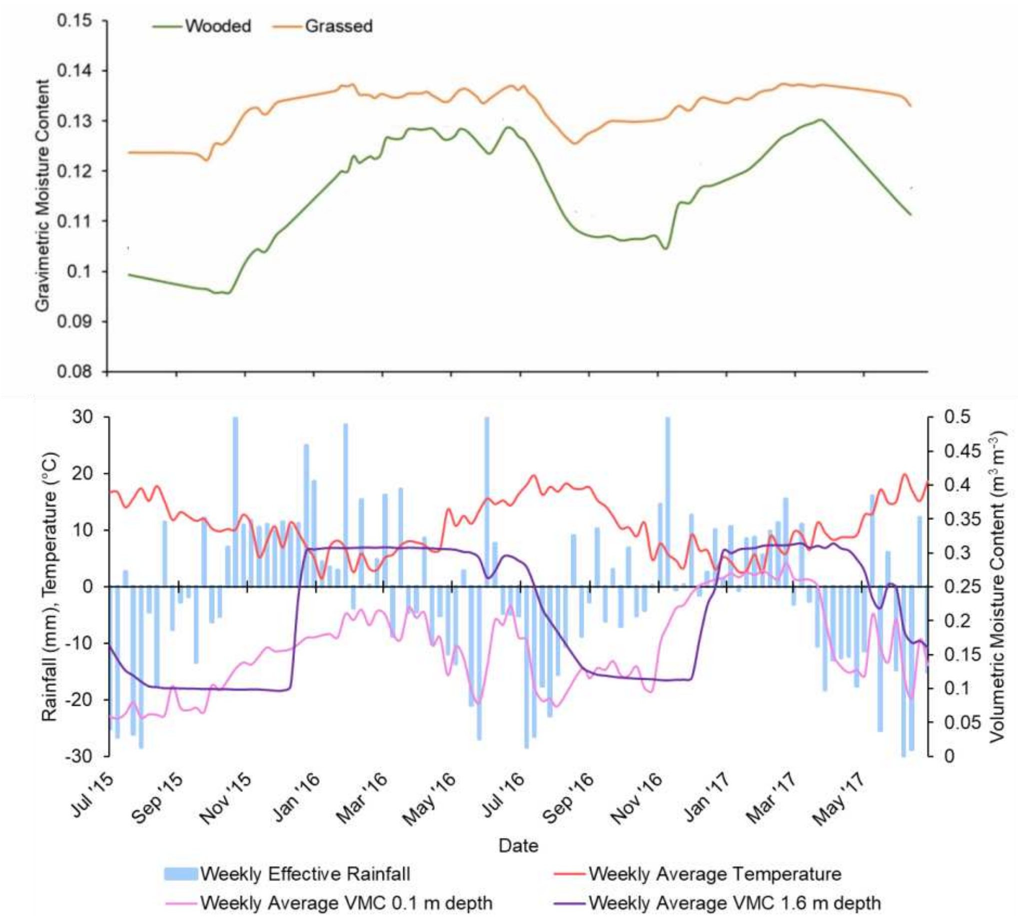

Figure 4: Weather data from Old Dalby field sensors, including rainfall data, temperature data and ground volumetric moisture content (VMC) data from sensors installed at 0.15 m depth and 2.6 m depth. This is shown beneath average gravimetric moisture content (GMC [g/g]) for the vegetated (wooded) and non-vegetated (grassed) areas of the slope (Holmes et al., in review).

4. Conclusions

The utility of a novel 4-D ERT system for slope monitoring has been demonstrated. In both field sites, hydrogeological responses to changing weather conditions were highlighted that cannot be observed using traditional techniques which are still the predominant methods of slope-monitoring currently deployed on transport networks. Calibration of ERT models from field monitoring with lab-derived petrophysical relationships enabled insight into subsurface moisture variations. Near-surface geophysics for slope monitoring provides stakeholders with a more complete understanding of the processes affecting slope stability to allow for a greater degree of confidence in decision-making regarding the management of slopes affecting transport infrastructure.

At each site, different controls on the changes in resistivity are identified. The response of the subsurface to changing weather conditions is controlled to a greater extent by temperature than by rainfall at the Ripley Landslide. The greatest changes are seen seasonally, with resistivity responding strongly to the influence of snowmelt as a result of fluctuating surface temperatures. At the Old Dalby site there is a spatial disparity in the seasonal response to changing weather conditions in wooded and grassed areas of the slope. The resistivity of grassed areas did not change significantly over time, whereas the resistivity of wooded areas was much higher in summer than in winter owing to greater plant activity during summer. As such, vegetation type is an important consideration for asset management on the transport network.

Acknowledgements

This research is a collaborative effort between Newcastle University, the British Geological Survey (BGS), The Geological Survey of Canada, and University College Dublin. BGS authors publish with permission of the Executive Director of the BGS (UKRI). The first author was funded by the Department for the Economy, Northern Ireland and the BGS. The BGS contribution is linked to the ACHILLES project (grant reference EP/R034575/1). The last author, Donohue, was funded by Science Foundation Ireland.

References

Chambers, J. E., Gunn, D. A., Wilkinson, P. B., Meldrum, P. I., Haslam, E., Holyoake, S., Kirkham, M., Juras, O., Merritt, A., Wragg, J. (2014) 4D electrical resistivity tomography monitoring of soil moisture dynamics in an operational railway embankment. *Near Surface Geophysics*. 12. 61-72.

Fredlund, D, G., Morgenstern, N, R., Widger, R. A. (1978) The shear strength of unsaturated soil. *Canadian Geotechnical Journal*. 15. 313-321.

Gunn, D. A., Chambers, J. E., Uhlemann, S., Wilkinson, P. B., Meldrum, P. I., Dijkstra, T. A., Haslam, E., Kirkham, M., Wragg, J., Holyoake, S., Hughes, P. N., HenJones, R., Glendinning, S. (2015) Moisture monitoring in clay embankments using electrical resistivity tomography. *Construction and Building Materials*. 92. 82-94.

Hayley, K., Bentley, L. R., Gharibi, M. & Nightingale, M. (2007) Low temperature dependence of electrical resistivity: Implications for near surface geophysical monitoring. *Geophysical Research Letters*. 34 (18).

Holmes, J., Chambers, J., Meldrum, P., Wilkinson, P., Boyd, J., Williamson, P., Huntley, D., Sattler, K., Elwood, D., Sivakumar, V., Reeves, H., Donohue, S. (2020) 4-Dimensional Electrical Resistivity Tomography for continuous, near real time monitoring of a landslide affecting transport infrastructure in British Columbia, Canada. *Near Surface Geophysics*. 18 (4).

Holmes, J., Chambers, J., Wilkinson, P., Meldrum, P., Cimpoiasu, M., Boyd, J., Huntley, D., Williamson, P., Gunn, D., Dashwood, B., Whiteley, J., Watlet, A., Kirkham, M., Sattler, K., Elwood, D., Sivakumar, V., Reeves, H., Donohue, S. (2022) Application of petrophysical relationships to electrical resistivity models for assessing the stability of a landslide in British Columbia, Canada. *Engineering Geology*. 301. 106613.

Holmes, J., Chambers, J., Wilkinson, P., Dashwood, B., Gunn, D., Cimpoiaşu, M., Kirkham, M., Uhlemann, S., Meldrum, P., Kuras, O., Huntley, D., Abbott, S., Sivakumar, V., Donohue, S. 4D electrical resistivity tomography for assessing the influence of vegetation and subsurface moisture on railway cutting condition. In Review. *Engineering Geology*.

Khan, S., Ivoke, J. & Nobahar, M. (2019) Coupled Effect of Wet-Dry Cycles and Rainfall on Highway Slope Made of Yazoo Clay. *Geosciences*, 9, 341.

Mair, R., Hight, D., McGinnity, B. (2021) *A Review of Earthworks Management*. Network Rail. Pp 543.

Mattsson, L-G., and Jenelius, E. (2015) Vulnerability and resilience of transport systems – A discussion of recent research. *Transportation Research Part A: Policy and Practice*. 81. 16-34.

Perrone, A., Lapenna, V. & Piscitelli, S. (2014) Electrical Resistivity Tomography Technique For Landslide Investigation: A Review. *Earth-Science Reviews*.135, 65-82.

Tso, C. H. M., Kuras, O., Wilkinson, P. B., Uhlemann, S., Chambers, J. E., Meldrum, P. I., Graham, J., Sherlock, E.F., Binley, A. (2017) Improved characterisation and modelling of measurement errors in electrical resistivity tomography (ERT) surveys. *Journal of Applied Geophysics*. 146. 103-119.

Uhlemann, S., Chambers, J., Wilkinson, P., Maurer, H., Merritt, A., Meldrum, P., Kuras, O., Gunn, D., Smith, A., Dijkstra, T. (2017) Four-dimensional imaging of moisture dynamics during landslide reactivation. *Journal of Geophysical Research: Earth Surface*. 122 (1). 398-418

Waxman, M. H. and Smits, L. J. M. (1968) Electrical conductivities in oil-bearing shaly sands. *Society of Petroleum Engineers* Journal. 8. 107-122.